

Measurement of exclusive ω electroproduction at HERA

ZEUS Collaboration

Abstract

The exclusive electroproduction of ω mesons, $ep \rightarrow e\omega p$, has been studied in the kinematic range $3 < Q^2 < 20 \text{ GeV}^2$, $40 < W < 120 \text{ GeV}$ and $|t| < 0.6 \text{ GeV}^2$ with the ZEUS detector at HERA using an integrated luminosity of 37.7 pb^{-1} . The ω mesons were identified via the decay $\omega \rightarrow \pi^+\pi^-\pi^0$. The exclusive cross section in the above kinematic region is $\sigma_{ep \rightarrow e\omega p} = 0.108 \pm 0.014(\text{stat.}) \pm 0.026(\text{syst.}) \text{ nb}$. The reaction $ep \rightarrow e\phi p$, $\phi \rightarrow \pi^+\pi^-\pi^0$, has also been measured. The cross sections, as well as the ratios $\sigma_{\gamma^*p \rightarrow \omega p} / \sigma_{\gamma^*p \rightarrow \rho^0 p}$ and $\sigma_{\gamma^*p \rightarrow \omega p} / \sigma_{\gamma^*p \rightarrow \phi p}$, are presented as a function of W and Q^2 . Thus, for the first time, the properties of ω electroproduction can be compared to those of ρ^0 , ϕ and J/ψ electroproduction at high W .

The ZEUS Collaboration

J. Breitweg, S. Chekanov, M. Derrick, D. Krakauer, S. Magill, B. Musgrave, A. Pellegrino, J. Repond, R. Stanek, R. Yoshida

Argonne National Laboratory, Argonne, IL, USA ^p

M.C.K. Mattingly

Andrews University, Berrien Springs, MI, USA

G. Abbiendi, F. Anselmo, P. Antonioli, G. Bari, M. Basile, L. Bellagamba, D. Boscherini¹, A. Bruni, G. Bruni, G. Cara Romeo, G. Castellini², L. Cifarelli³, F. Cindolo, A. Contin, N. Coppola, M. Corradi, S. De Pasquale, P. Giusti, G. Iacobucci, G. Laurenti, G. Levi, A. Margotti, T. Massam, R. Nania, F. Palmonari, A. Pesci, A. Polini, G. Sartorelli, Y. Zamora Garcia⁴, A. Zichichi

University and INFN Bologna, Bologna, Italy ^f

C. Amelung, A. Bornheim⁵, I. Brock, K. Coböken⁶, J. Crittenden, R. Deffner⁷, H. Hartmann, K. Heinloth, E. Hilger, P. Irrgang, H.-P. Jakob, A. Kappes, U.F. Katz, R. Kerger, E. Paul, J. Rautenberg, H. Schnurbusch, A. Stifutkin, J. Tandler, K.C. Voss, A. Weber, H. Wieber

Physikalisches Institut der Universität Bonn, Bonn, Germany ^c

D.S. Bailey, O. Barret, N.H. Brook⁸, B. Foster¹, G.P. Heath, H.F. Heath, J.D. McFall, E. Rodrigues, J. Scott, R.J. Tapper

H.H. Wills Physics Laboratory, University of Bristol, Bristol, U.K. ^o

M. Capua, A. Mastroberardino, M. Schioppa, G. Susinno

Calabria University, Physics Dept.and INFN, Cosenza, Italy ^f

H.Y. Jeoung, J.Y. Kim, J.H. Lee, I.T. Lim, K.J. Ma, M.Y. Pac⁹

Chonnam National University, Kwangju, Korea ^h

A. Caldwell, W. Liu, X. Liu, B. Mellado, S. Paganis, S. Sampson, W.B. Schmidke, F. Sciulli

Columbia University, Nevis Labs., Irvington on Hudson, N.Y., USA ^q

J. Chwastowski, A. Eskreys, J. Figiel, K. Klimek, K. Olkiewicz, K. Piotrkowski¹⁰, M.B. Przybycień, P. Stopa, L. Zawiejski

Inst. of Nuclear Physics, Cracow, Poland ^j

B. Bednarek, K. Jeleń, D. Kisieleska, A.M. Kowal, T. Kowalski, M. Przybycień, E. Rulikowska-Zarębska, L. Suszycki, D. Szuba

Faculty of Physics and Nuclear Techniques, Academy of Mining and Metallurgy, Cracow, Poland ^j

A. Kotański

Jagellonian Univ., Dept. of Physics, Cracow, Poland ^k

L.A.T. Bauerdick, U. Behrens, J.K. Bienlein, K. Borras, D. Dannheim, K. Desler, G. Drews, A. Fox-Murphy, U. Fricke, F. Goebel, S. Goers, P. Göttlicher, R. Graciani, T. Haas, W. Hain, G.F. Hartner, D. Hasell¹¹, K. Hebbel, M. Kasemann¹², W. Koch, U. Kötz, H. Kowalski, L. Lindemann¹³, B. Löhr, R. Mankel, M. Martínez, M. Milite, M. Moritz, D. Notz, F. Pelucchi, M.C. Petrucci, M. Rohde, A.A. Savin, U. Schneekloth, F. Selonke, M. Sievers¹⁴, S. Stonjek, G. Wolf, U. Wollmer, C. Youngman, W. Zeuner
Deutsches Elektronen-Synchrotron DESY, Hamburg, Germany

C. Coldewey, A. Lopez-Duran Viani, A. Meyer, S. Schlenstedt, P.B. Straub
DESY Zeuthen, Zeuthen, Germany

G. Barbagli, E. Gallo, P. Pelfer
University and INFN, Florence, Italy^f

G. Maccarrone, L. Votano
INFN, Laboratori Nazionali di Frascati, Frascati, Italy^f

A. Bamberger, A. Benen, S. Eisenhardt¹⁵, P. Markun, H. Raach, S. Wölffe
Fakultät für Physik der Universität Freiburg i.Br., Freiburg i.Br., Germany^c

P.J. Bussey, M. Bell, A.T. Doyle, S.W. Lee, A. Lupi, N. Macdonald, G.J. McCance, D.H. Saxon, L.E. Sinclair, I.O. Skillicorn, R. Waugh
Dept. of Physics and Astronomy, University of Glasgow, Glasgow, U.K.^o

I. Bohnet, N. Gendner, U. Holm, A. Meyer-Larsen, H. Salehi, K. Wick
Hamburg University, I. Institute of Exp. Physics, Hamburg, Germany^c

A. Garfagnini, I. Gialas¹⁶, L.K. Gladilin¹⁷, D. Kçira¹⁸, R. Klanner, E. Lohrmann, G. Poelz, F. Zetsche
Hamburg University, II. Institute of Exp. Physics, Hamburg, Germany^c

R. Goncalo, K.R. Long, D.B. Miller, A.D. Tapper, R. Walker
Imperial College London, High Energy Nuclear Physics Group, London, U.K.^o

U. Mallik
University of Iowa, Physics and Astronomy Dept., Iowa City, USA^p

P. Cloth, D. Filges
Forschungszentrum Jülich, Institut für Kernphysik, Jülich, Germany

T. Ishii, M. Kuze, K. Nagano, K. Tokushuku¹⁹, S. Yamada, Y. Yamazaki
Institute of Particle and Nuclear Studies, KEK, Tsukuba, Japan^q

S.H. Ahn, S.B. Lee, S.K. Park
Korea University, Seoul, Korea^h

H. Lim, I.H. Park, D. Son
Kyungpook National University, Taegu, Korea^h

F. Barreiro, G. García, C. Glasman²⁰, O. González, L. Labarga, J. del Peso, I. Redondo²¹, J. Terrón
*Univer. Autónoma Madrid, Depto de Física Teórica, Madrid, Spain*ⁿ

M. Barbi, F. Corriveau, D.S. Hanna, A. Ochs, S. Padhi, D.G. Stairs, M. Wing
McGill University, Dept. of Physics, Montréal, Québec, Canada^{a, b}

T. Tsurugai
Meiji Gakuin University, Faculty of General Education, Yokohama, Japan

A. Antonov, V. Bashkirov²², M. Danilov, B.A. Dolgoshein, D. Gladkov, V. Sosnovtsev,
S. Suchkov
Moscow Engineering Physics Institute, Moscow, Russia^l

R.K. Dementiev, P.F. Ermolov, Yu.A. Golubkov, I.I. Katkov, L.A. Khein, N.A. Korotkova,
I.A. Korzhavina, V.A. Kuzmin, O.Yu. Lukina, A.S. Proskuryakov, L.M. Shcheglova,
A.N. Solomin, N.N. Vlasov, S.A. Zotkin
Moscow State University, Institute of Nuclear Physics, Moscow, Russia^m

C. Bokel, M. Botje, N. Brümmer, J. Engelen, S. Grijpink, E. Koffeman, P. Kooijman,
S. Schagen, A. van Sighem, E. Tassi, H. Tiecke, N. Tuning, J.J. Velthuis, J. Vossebeld,
L. Wiggers, E. de Wolf
*NIKHEF and University of Amsterdam, Amsterdam, Netherlands*ⁱ

B. Bylsma, L.S. Durkin, J. Gilmore, C.M. Ginsburg, C.L. Kim, T.Y. Ling
Ohio State University, Physics Department, Columbus, Ohio, USA^p

S. Boogert, A.M. Cooper-Sarkar, R.C.E. Devenish, J. Große-Knetter²³, T. Matsushita,
O. Ruske, M.R. Sutton, R. Walczak
Department of Physics, University of Oxford, Oxford U.K.^o

A. Bertolin, R. Brugnera, R. Carlin, F. Dal Corso, U. Dosselli, S. Dusini, S. Limentani,
M. Morandin, M. Posocco, L. Stanco, R. Stroili, M. Turcato, C. Voci
Dipartimento di Fisica dell'Università and INFN, Padova, Italy^f

L. Adamczyk²⁴, L. Iannotti²⁴, B.Y. Oh, J.R. Okrasinski, P.R.B. Saull²⁴, W.S. Toothacker²⁵†,
J.J. Whitmore
Pennsylvania State University, Dept. of Physics, University Park, PA, USA^q

Y. Iga
Polytechnic University, Sagami-hara, Japan^g

G. D'Agostini, G. Marini, A. Nigro
Dipartimento di Fisica, Univ. 'La Sapienza' and INFN, Rome, Italy^f

C. Cormack, J.C. Hart, N.A. McCubbin, T.P. Shah
Rutherford Appleton Laboratory, Chilton, Didcot, Oxon, U.K.^o

D. Epperson, C. Heusch, H.F.-W. Sadrozinski, A. Seiden, R. Wichmann, D.C. Williams
University of California, Santa Cruz, CA, USA^p

N. Pavel
Fachbereich Physik der Universität-Gesamthochschule Siegen, Germany^c

H. Abramowicz²⁶, S. Dagan²⁷, S. Kananov²⁷, A. Kreisel, A. Levy²⁷
*Raymond and Beverly Sackler Faculty of Exact Sciences, School of Physics, Tel-Aviv
University, Tel-Aviv, Israel*^e

T. Abe, T. Fusayasu, K. Umemori, T. Yamashita
Department of Physics, University of Tokyo, Tokyo, Japan^g

R. Hamatsu, T. Hirose, M. Inuzuka, S. Kitamura²⁸, T. Nishimura
Tokyo Metropolitan University, Dept. of Physics, Tokyo, Japan^g

M. Arneodo²⁹, N. Cartiglia, R. Cirio, M. Costa, M.I. Ferrero, S. Maselli, V. Monaco,
C. Peroni, M. Ruspa, R. Sacchi, A. Solano, A. Staiano
Università di Torino, Dipartimento di Fisica Sperimentale and INFN, Torino, Italy^f

M. Dardo
II Faculty of Sciences, Torino University and INFN - Alessandria, Italy^f

D.C. Bailey, C.-P. Fagerstroem, R. Galea, T. Koop, G.M. Levman, J.F. Martin, R.S. Orr,
S. Polenz, A. Sabetfakhri, D. Simmons
University of Toronto, Dept. of Physics, Toronto, Ont., Canada^a

J.M. Butterworth, C.D. Catterall, M.E. Hayes, E.A. Heaphy, T.W. Jones, J.B. Lane,
B.J. West
University College London, Physics and Astronomy Dept., London, U.K.^o

J. Ciborowski, R. Ciesielski, G. Grzelak, R.J. Nowak, J.M. Pawlak, R. Pawlak, B. Smal-
ska, T. Tymieniecka, A.K. Wróblewski, J.A. Zakrzewski, A.F. Żarnecki
Warsaw University, Institute of Experimental Physics, Warsaw, Poland^j

M. Adamus, T. Gadaj
Institute for Nuclear Studies, Warsaw, Poland^j

O. Deppe, Y. Eisenberg, D. Hochman, U. Karshon²⁷
Weizmann Institute, Department of Particle Physics, Rehovot, Israel^d

W.F. Badgett, D. Chapin, R. Cross, C. Foudas, S. Mattingly, D.D. Reeder, W.H. Smith,
A. Vaiciulis³⁰, T. Wildschek, M. Wodarczyk
University of Wisconsin, Dept. of Physics, Madison, WI, USA^p

A. Deshpande, S. Dhawan, V.W. Hughes
Yale University, Department of Physics, New Haven, CT, USA^p

S. Bhadra, C. Catterall, J.E. Cole, W.R. Frisken, R. Hall-Wilton, M. Khakzad, S. Menary
York University, Dept. of Physics, Toronto, Ont., Canada^a

¹ now visiting scientist at DESY
² also at IROE Florence, Italy
³ now at Univ. of Salerno and INFN Napoli, Italy
⁴ supported by Worldlab, Lausanne, Switzerland
⁵ now at CalTech, USA
⁶ now at Sparkasse Bonn, Germany
⁷ now at Siemens ICN, Berlin, Germany
⁸ PPARC Advanced fellow
⁹ now at Dongshin University, Naju, Korea
¹⁰ now at CERN
¹¹ now at Massachusetts Institute of Technology, Cambridge, MA, USA
¹² now at Fermilab, Batavia, IL, USA
¹³ now at SAP A.G., Walldorf, Germany
¹⁴ now at SuSE GmbH, Nürnberg, Germany
¹⁵ now at University of Edinburgh, Edinburgh, U.K.
¹⁶ visitor of Univ. of Crete, Greece, partially supported by DAAD, Bonn - Kz. A/98/16764
¹⁷ on leave from MSU, supported by the GIF, contract I-0444-176.07/95
¹⁸ supported by DAAD, Bonn - Kz. A/98/12712
¹⁹ also at University of Tokyo
²⁰ supported by an EC fellowship number ERBFMBICT 972523
²¹ supported by the Comunidad Autonoma de Madrid
²² now at Loma Linda University, Loma Linda, CA, USA
²³ supported by the Feodor Lynen Program of the Alexander von Humboldt foundation
²⁴ partly supported by Tel Aviv University
²⁵ deceased
²⁶ an Alexander von Humboldt Fellow at University of Hamburg
²⁷ supported by a MINERVA Fellowship
²⁸ present address: Tokyo Metropolitan University of Health Sciences, Tokyo 116-8551,
 Japan
²⁹ now also at Università del Piemonte Orientale, I-28100 Novara, Italy
³⁰ now at University of Rochester, Rochester, NY, USA

- ^a supported by the Natural Sciences and Engineering Research Council of Canada (NSERC)
- ^b supported by the FCAR of Québec, Canada
- ^c supported by the German Federal Ministry for Education and Science, Research and Technology (BMBF), under contract numbers 057BN19P, 057FR19P, 057HH19P, 057HH29P, 057SI75I
- ^d supported by the MINERVA Gesellschaft für Forschung GmbH, the German Israeli Foundation, the Israel Science Foundation, the Israel Ministry of Science and the Benozio Center for High Energy Physics
- ^e supported by the German-Israeli Foundation, the Israel Science Foundation, the U.S.-Israel Binational Science Foundation, and by the Israel Ministry of Science
- ^f supported by the Italian National Institute for Nuclear Physics (INFN)
- ^g supported by the Japanese Ministry of Education, Science and Culture (the Monbusho) and its grants for Scientific Research
- ^h supported by the Korean Ministry of Education and Korea Science and Engineering Foundation
- ⁱ supported by the Netherlands Foundation for Research on Matter (FOM)
- ^j supported by the Polish State Committee for Scientific Research, grant No. 112/E-356/SPUB/DESY/P03/DZ 3/99, 620/E-77/SPUB/DESY/P-03/ DZ 1/99, 2P03B03216, 2P03B04616, 2P03B03517, and by the German Federal Ministry of Education and Science, Research and Technology (BMBF)
- ^k supported by the Polish State Committee for Scientific Research (grant No. 2P03B08614 and 2P03B06116)
- ^l partially supported by the German Federal Ministry for Education and Science, Research and Technology (BMBF)
- ^m supported by the Fund for Fundamental Research of Russian Ministry for Science and Education and by the German Federal Ministry for Education and Science, Research and Technology (BMBF)
- ⁿ supported by the Spanish Ministry of Education and Science through funds provided by CICYT
- ^o supported by the Particle Physics and Astronomy Research Council
- ^p supported by the US Department of Energy
- ^q supported by the US National Science Foundation

1 Introduction

The exclusive photoproduction of vector mesons, ρ^0 , ω , ϕ and J/ψ , has been studied over a wide range of the photon-proton centre-of-mass energy W [1–8]. For high W and for light vector mesons, these reactions display features characteristic of soft diffractive processes, and are well described within the framework of the vector dominance model (VDM) [9] and Regge phenomenology [10]. In the VDM, the photon is assumed to fluctuate into a vector meson (VM), which subsequently interacts with the target proton. The expectation of the VDM and Regge phenomenology is that the cross sections for exclusive VM production will be in proportions determined by the couplings of the photon to the vector mesons and by the elastic VM-proton cross sections. The couplings, in particular, are determined by the quark current decomposition of the photon and by the quark wave function of the VM. The SU(4) prediction, which ignores the VM mass differences, is that the coupling strengths of the photon to the ρ^0 , ω , ϕ and J/ψ mesons are in the ratio¹ 9:1:2:8. Both at fixed target experiments at $W \gtrsim 8$ GeV [1] and at HERA [5–7], the ratio ω/ρ^0 of the exclusive photoproduction cross sections is found to be approximately 1:9, while the ϕ/ρ^0 and $(J/\psi)/\rho^0$ ratios are found to be smaller than the SU(4) predicted ratios of photon-VM couplings.

For high-energy exclusive photoproduction of heavy VMs and for electroproduction of all VMs at large virtualities, Q^2 , of the exchanged virtual photon, γ^* , an alternative production mechanism has been proposed [11–13]: the virtual photon fluctuates into a $q\bar{q}$ pair before arriving at the target, and it is this $q\bar{q}$ state that scatters elastically off the proton. The VM is formed well after the interaction. If the transverse size of the $q\bar{q}$ fluctuation is small enough, the interaction is expected to become flavour independent and the gluons of the proton are resolved [14]. Such a configuration occurs when the mass of the quarks is large or if the photon with large virtuality is longitudinally polarized. In these cases, perturbative QCD can be applied [11, 12, 15–17] and the expectation for the ratios of VM production cross sections is given by the ratios of the couplings.

The HERA measurements of exclusive electroproduction of ρ^0 [18, 19], ϕ [20, 21] and J/ψ [18, 22] mesons, as well as the exclusive photoproduction of J/ψ [7, 8] and Υ [8, 23] mesons, are in broad agreement with the expectations from QCD. In particular, the sharp decrease of the cross sections with Q^2 , the strong rise of the J/ψ cross section with W , the change in the W dependence and the broadening of the t distribution of the ρ^0 cross section with increasing Q^2 show the expected behaviour. With increasing Q^2 , the ϕ/ρ^0 and $(J/\psi)/\rho^0$ cross-section ratios rise towards the expected values.

This letter reports the first measurement of the exclusive ω electroproduction cross section for $40 < W < 120$ GeV and $3 < Q^2 < 20$ GeV². The ω mesons were identified via the decay $\omega \rightarrow \pi^+\pi^-\pi^0$. Measurements of the exclusive ϕ electroproduction cross section using the $\pi^+\pi^-\pi^0$ final state are also reported. The compatibility of the ω/ρ^0 and ω/ϕ cross-section ratios with the SU(4) hypothesis is investigated. Thus, the data presented here permits, for the first time, a discussion of the ratios of the production cross sections of all VMs related by SU(4).

¹If the coupling strengths are calculated from the VM masses and the measured partial widths, $\Gamma_{V \rightarrow e^+e^-}$, the ratio becomes 9:0.8:2.4:28

2 Experimental conditions

The measurements were performed at the ep collider HERA with the ZEUS detector using an integrated luminosity of 37.7 pb^{-1} . During 1996 and 1997 HERA operated with a proton energy of 820 GeV and a positron energy of 27.5 GeV. A detailed description of the ZEUS detector can be found elsewhere [24]. The main components used in this analysis are described below.

The high-resolution uranium-scintillator calorimeter CAL [25] consists of three parts: forward² (FCAL), barrel (BCAL) and rear (RCAL) calorimeters. Each part is subdivided transversely into towers, which are segmented longitudinally into one electromagnetic section (EMC) and one (RCAL) or two (FCAL, BCAL) hadronic sections (HAC). Each section is further subdivided into cells, which are the units that are read out. The relative energy resolutions of the calorimeter, as determined in a test beam, are $\sigma_E/E = 0.18/\sqrt{E}$ for electrons and $\sigma_E/E = 0.35/\sqrt{E}$ for hadrons, where E is expressed in GeV.

Charged-particle tracks are reconstructed and their momenta determined using the central tracking detector (CTD) [26]. The CTD is a cylindrical drift chamber operated in a magnetic field of 1.43 T produced by a thin superconducting solenoid. The CTD consists of 72 cylindrical layers, organised in 9 superlayers covering the polar angular region $15^\circ < \theta < 164^\circ$. The transverse momentum resolution for full-length tracks is $\sigma_{p_\perp}/p_\perp = 0.0058 p_\perp \oplus 0.0065 \oplus 0.0014/p_\perp$ (p_\perp in GeV).

The positions of positrons scattered at small angles with respect to the beam direction are determined by the small-angle rear tracking detector (SRTD). The SRTD is attached to the front face of the RCAL. It consists of two planes of scintillator strips, 1 cm wide and 0.5 cm thick, arranged in orthogonal orientations and read out via optical fibres and photomultiplier tubes. It covers the region of $68 \times 68 \text{ cm}^2$ in X and Y , except for a $10 \times 20 \text{ cm}^2$ hole at the centre for the beam pipe. The SRTD has a position resolution of 0.3 cm.

The luminosity is determined from the rate of the Bethe-Heitler process $e^+p \rightarrow e^+\gamma p$, where the high-energy photon is detected in a lead-scintillator calorimeter located at $Z = -107 \text{ m}$ in the HERA tunnel downstream of the interaction point in the positron flight direction [27].

3 Kinematics and cross sections

Figure 1 shows a schematic diagram for the reaction:

$$e(k) p(P) \rightarrow e(k') V(v) p(P')$$

where V is an ω or ϕ meson and k, k', P, P' , and v are the four-momenta of the incident positron, scattered positron, incident proton, scattered proton and vector meson, respectively. The kinematic variables used to describe exclusive VM production are:

- $Q^2 = -q^2 = -(k - k')^2$, the negative squared four-momentum of the virtual photon;

²Throughout this paper the standard ZEUS right-handed coordinate system is used: the Z -axis points in the direction of the proton beam momentum (referred to as the forward direction) and the horizontal X -axis points towards the centre of HERA. The nominal interaction point is at $X = Y = Z = 0$. The polar angle θ is defined with respect to the positive Z -direction.

- $W^2 = (q + P)^2$, the squared centre-of-mass energy of the photon-proton system;
- $y = (P \cdot q)/(P \cdot k)$, the fraction of the positron energy transferred to the photon in the proton rest frame;
- $t = (P - P')^2 = (v - q)^2$, the squared four-momentum-transfer at the proton vertex.

The kinematic variables were reconstructed using the “constrained” method. This method uses the momenta of the decay charged particles measured in the CTD, the momenta of the two photons from the $\pi^0 \rightarrow \gamma\gamma$ decay, measured as described in Section 5, and the polar and azimuthal angles of the scattered positron measured by the CAL and the SRTD. Neglecting the transverse momentum of the outgoing proton with respect to its incoming momentum, the energy of the scattered positron can be expressed as:

$$E_{e'} \simeq [2E_e - (E_V - p_V^Z)]/(1 - \cos \theta_{e'})$$

where E_e is the energy of the incident positron, E_V and p_V^Z are the energy and longitudinal momentum of the vector meson V , and $\theta_{e'}$ is the polar angle of the scattered positron. The value of Q^2 was calculated from:

$$Q^2 = 2E_{e'}E_e(1 + \cos \theta_{e'})$$

and W and t were calculated as described above.

In the Born approximation, the virtual photon-proton cross section, σ^{γ^*p} , can be determined from the measured positron-proton cross section:

$$\sigma^{\gamma^*p} = \sigma_T^{\gamma^*p} + \epsilon\sigma_L^{\gamma^*p} = \frac{1}{\Gamma_T(Q^2, y)} \cdot \frac{d^2\sigma^{ep}}{dQ^2 dy}$$

where $\epsilon = 2(1 - y)/[1 + (1 - y)^2]$, Γ_T is the flux of transverse photons and $\sigma_T^{\gamma^*p}$ and $\sigma_L^{\gamma^*p}$ are the transverse and the longitudinal virtual photoproduction cross sections, respectively. The cross-section σ^{γ^*p} is used to evaluate the total exclusive cross section, $\sigma_{\text{tot}}^{\gamma^*p} = \sigma_T^{\gamma^*p} + \sigma_L^{\gamma^*p}$, through the relation:

$$\sigma_{\text{tot}}^{\gamma^*p} = \frac{1 + R}{1 + \epsilon R} \sigma^{\gamma^*p}$$

where $R = \sigma_L^{\gamma^*p}/\sigma_T^{\gamma^*p}$. In the kinematic range of this measurement, the value of ϵ is close to unity, and σ^{γ^*p} differs from $\sigma_{\text{tot}}^{\gamma^*p}$ by less than one percent.

4 Event selection

Events were selected online with a three-level trigger system. Offline, the following requirements were imposed to select candidates for the reaction $e^+p \rightarrow e^+\pi^+\pi^-\pi^0p$:

- the energy of the scattered positron, measured in the CAL, was required to be greater than 10 GeV;

- the interaction vertex was required to have its Z coordinate within ± 50 cm of the nominal interaction point and to lie within a transverse distance of 0.6 cm of the nominal beam position;
- in addition to a scattered positron, two oppositely charged tracks were required, each associated with the reconstructed vertex, and each with pseudorapidity³ $|\eta| < 1.75$ and transverse momentum greater than 150 MeV;
- in addition to the energy deposits in the calorimeter matched to the scattered positron and to the above-mentioned tracks, two further electromagnetic energy deposits in the calorimeter were required (see Section 5);
- to suppress the contribution from proton dissociation (see Section 7), events with energy deposits above 800 MeV in the forward calorimeter within a radius of 50 cm from the Z axis were rejected;
- to reduce the corrections from initial-state radiation, a cut on the difference in total energy and total longitudinal momentum, as measured in the CAL, of $E - p_Z > 40$ GeV was applied.

In addition, the following cuts were applied to select a kinematic region of high acceptance: $3 < Q^2 < 20$ GeV², $40 < W < 120$ GeV and $|t| < 0.6$ GeV². Only events in the $\pi^+\pi^-$ mass interval $0.3 < M_{\pi\pi} < 0.6$ GeV were kept for further analysis.

5 Reconstruction of the π^0

The two-photon decay of the π^0 was reconstructed using signals in the calorimeter combined into condensates, which are objects consisting of adjacent calorimeter cells. To reject background from uranium radioactivity in the calorimeter cells, a minimum individual cell energy of 100 MeV was required. Only condensates consisting solely of cells in the EMC section of the CAL were used. The position and energy, E_γ , of these condensates were then used to determine the invariant mass, $M_{\gamma\gamma}$, of the photon candidates, assuming the event vertex as measured by the CTD.

Uranium noise and CAL cells not correctly matched to charged tracks can yield condensates which are misidentified as low-energy photons. Such condensates introduce a background contribution to the $M_{\gamma\gamma}$ spectrum and were largely removed by requiring a minimum photon energy of 200 MeV and $E_{\gamma 1} + E_{\gamma 2} > 600$ MeV, where $\gamma 1$ is the more energetic photon. These energy requirements reduced the acceptance of the analysis by a factor of two, but reduced the systematic uncertainty on the background subtraction by a factor of three. The quantity $|E_{\gamma 1} - E_{\gamma 2}|/(E_{\gamma 1} + E_{\gamma 2})$, which is particularly sensitive to backgrounds, is shown in Fig. 2a. The data and the Monte Carlo (MC) simulation described in Section 6 agree well after the above requirements are applied. The resulting $M_{\gamma\gamma}$ spectrum is shown in Fig. 2b, where a clear π^0 mass peak is seen. A fit to the sum of a Gaussian function and a second-order polynomial yielded a mean value of the Gaussian of 110 ± 2 MeV, in good agreement with simulation studies of the detector response. The difference with respect to the nominal π^0 mass is mainly due to the energy loss in the superconducting solenoid in front of the calorimeter and was implicitly corrected for

³The pseudorapidity η is defined as $\eta = -\ln[\tan(\frac{\theta}{2})]$.

by the fit explained below. Only events with $M_{\gamma\gamma} < 200$ MeV were retained for further analysis.

To improve the resolution in the momentum of the $\pi^+\pi^-\pi^0$ system, the invariant mass of the two photons was constrained to the π^0 mass. The angle α between the two photons is well determined by the position information of the condensates, so that the resolution in $M_{\gamma\gamma}$ is dominated by the energy resolution. Thus, only the energies of the photons were varied in this procedure. The modified values $E_{\gamma 1}^{\text{fit}}$, $E_{\gamma 2}^{\text{fit}}$ of the energies $E_{\gamma 1}$, $E_{\gamma 2}$ of the CAL condensates were determined by minimising the quantity:

$$\chi^2(E_{\gamma 1}^{\text{fit}}, E_{\gamma 2}^{\text{fit}}) = \frac{(E_{\gamma 1} - E_{\gamma 1}^{\text{fit}})^2}{\sigma_{E_{\gamma 1}^{\text{fit}}}^2} + \frac{(E_{\gamma 2} - E_{\gamma 2}^{\text{fit}})^2}{\sigma_{E_{\gamma 2}^{\text{fit}}}^2}$$

using the constraint:

$$M_{\pi^0} = \sqrt{2 \cdot E_{\gamma 1}^{\text{fit}} E_{\gamma 2}^{\text{fit}} \cdot (1 - \cos \alpha)}$$

where $\sigma_{E_{\gamma i}^{\text{fit}}}(\text{GeV}) \propto \sqrt{E_{\gamma i}^{\text{fit}}(\text{GeV})}$ are the corresponding energy resolutions of the calorimeter.

6 Monte Carlo simulation and acceptance corrections

A MC generator for exclusive electroproduction of light VMs [28], interfaced to HERACLES [29] to simulate radiative effects, was used to evaluate the acceptance. In this generator the cross sections were parameterised over the entire W and Q^2 range using the ZEUS data on ρ^0 electroproduction [18] in terms of $\sigma_L^{\gamma^* p \rightarrow V p}$ and $\sigma_T^{\gamma^* p \rightarrow V p}$, where $V = \rho^0, \omega$ or ϕ ; s -channel helicity conservation was assumed. The MC samples generated in this way display good agreement with the present data, for both ω and ϕ production. Whenever the results of the current analysis are compared to previously published cross sections at slightly different values of Q^2 and W , the cross sections have been translated to appropriate values using the ZEUS ρ^0 cross-section parameterisation.

The average acceptance for ω mesons is 2.5%, an order of magnitude lower than that for the corresponding ZEUS ρ^0 analysis. This is mainly caused by the low π^0 reconstruction efficiency. The corresponding acceptance for ϕ mesons is 2.3%.

The Monte Carlo program DIPSI [30], based on the model of Ryskin [15], was used for systematic checks.

7 Background

The main source of resonant background to the exclusive reaction $ep \rightarrow eVp$ is the proton-dissociative reaction $ep \rightarrow eVN$, where N is a hadronic system produced by the dissociation of the proton. The proton-dissociative events in which the hadronic system N deposits energy around the beam pipe in the FCAL are removed by the selection criteria; the rest are misidentified as $ep \rightarrow eVp$ reactions and therefore have to be subtracted. The proton-dissociative fraction of events was estimated in the ZEUS ρ^0 analysis to be $(24_{-5}^{+9})\%$ for $|t| < 0.6 \text{ GeV}^2$, independent of Q^2 and W . The same fraction was assumed in this study.

8 Results

8.1 Analysis of the mass spectrum

The invariant-mass ($M_{3\pi}$) spectrum for the $\pi^+\pi^-\pi^0$ system after all offline cuts is shown in Fig. 3a. In addition to the ω signal, a second peak is visible from the process $ep \rightarrow e\phi p$ ($\phi \rightarrow \pi^+\pi^-\pi^0$). The spectrum was fitted with the function:

$$f(M_{3\pi}) = g_1(M_{3\pi}) + g_2(M_{3\pi}) + \zeta(M_{3\pi})$$

where g_1 and g_2 are Gaussian functions to describe the ω and ϕ mass peaks, and ζ is a second-order polynomial representing the background. The latter is mainly due to the background under the π^0 peak, as well as to other processes in which an $e\pi^+\pi^-\pi^0$ final state is detected. The fitted values of the ω and ϕ masses are 787 ± 5 MeV and 1019 ± 10 MeV, respectively, compatible with their nominal values [31] and with MC expectations. The values obtained for the widths are dominated by the detector resolution. The standard deviations of the Gaussian resolution functions are 38 MeV for the ω and 36 MeV for the ϕ , in accord with the MC predictions.

The number of ω and ϕ candidates observed after background subtraction was determined by integrating the corresponding Gaussian function, which yielded $N_\omega = 116 \pm 14$ and $N_\phi = 38 \pm 11$.

8.2 Cross sections and systematic uncertainties

The cross sections for the reaction $ep \rightarrow eVp$, where $V = \omega$ or ϕ , were determined using the expression:

$$\sigma_{ep \rightarrow eVp} = \frac{N_V \cdot \Delta}{A_V \cdot L \cdot B_V}$$

where N_V is the total number of observed events, L is the integrated luminosity, Δ is the correction for the proton-dissociation background, and A_V and B_V are the overall acceptance and branching ratio, respectively.

The systematic uncertainties are dominated by the uncertainty in the extraction of the number of ω or ϕ events and the uncertainty of the proton-dissociative background. The extraction of the number of events dominates the uncertainty because of the large number (nine) of free parameters needed to fit the mass distribution and the small number of signal events. When different $M_{\pi\pi}$ or $M_{\gamma\gamma}$ cuts were applied, the shape of the mass spectrum changed, which led to differences in the values of the fit parameters, and hence the number of resonant events. The systematic uncertainty due to this procedure for extracting the number of events is about 15%. The uncertainty in the proton-dissociative background was taken from the ZEUS ρ^0 analysis.

In the kinematic range $3 < Q^2 < 20$ GeV², $40 < W < 120$ GeV and $|t| < 0.6$ GeV², the ω and ϕ exclusive electroproduction cross sections are $\sigma_{ep \rightarrow e\omega p} = 0.108 \pm 0.014(stat.) \pm 0.026(syst.)$ nb and $\sigma_{ep \rightarrow e\phi p} = 0.220 \pm 0.064(stat.) \pm 0.077(syst.)$ nb. The corresponding γ^*p cross sections are presented in Table 1.

The measured cross sections for exclusive ω production as a function of W and Q^2 are presented in Figs. 3b and 3c. The corresponding values are given in Tables 2 and 3. The exclusive ω photoproduction data ($Q^2 \simeq 0$ GeV²) displayed in Fig. 3c were taken from a previous ZEUS publication [5]. The ρ^0 data [4,18] are also shown for comparison.

The measured Q^2 and W dependences for exclusive ω production are consistent with those for ρ^0 meson production [18].

8.3 Cross-section ratios

The ω/ϕ , ω/ρ^0 , and ϕ/ρ^0 cross-section ratios, obtained at $W = 70$ GeV for the whole data sample measured here, are listed in Table 1.

The ratio $\omega/\phi = 0.49 \pm 0.15(stat.) \pm 0.12(syst.)$, obtained with the present data, is consistent with the value expected from flavour independence. In this case, most of the systematic uncertainties are common to the ω and ϕ cross-section measurements and cancel in the ratio.

In Table 3 and Fig. 4, the ratios of the exclusive ω to ρ^0 production cross sections are shown for three Q^2 values. The ratio at $Q^2 \simeq 0$ GeV² was calculated using measured ω [5] and ρ^0 [4] photoproduction cross sections at $W = 80$ and $W = 75$ GeV, respectively, whereas the ratios at higher Q^2 are for $W = 70$ GeV. Due to the weak W dependence in photoproduction, a direct comparison can be made without correction. No Q^2 dependence of the ω/ρ^0 cross-section ratio is observed. The ratio is consistent with the value expected from flavour independence.

The ϕ/ρ^0 cross-section ratio from Table 1 is shown in Fig. 4. Also shown in Fig. 4 are the H1 data at $Q^2 > 1$ GeV² [21] and ZEUS data at $Q^2 \simeq 0$ GeV² [6] and $Q^2 = 12.3$ GeV² [20], all obtained using the $\phi \rightarrow K^+K^-$ channel. The present result is consistent with the earlier measurements. The ϕ/ρ^0 ratio approaches the SU(4) value for $Q^2 \gtrsim 6$ GeV².

For both the ω/ρ^0 and the ϕ/ρ^0 cross-section ratios presented in this paper, the systematic uncertainties on the subtraction of the proton-dissociative background cancel in the ratios. The remaining systematic uncertainties were assumed to be dominated by the uncertainties on the ω and ϕ cross section measurements.

For completeness, the $(J/\psi)/\rho^0$ cross-section ratios⁴ at $W = 90$ GeV [7, 18] are displayed in Fig. 4. A clear increase of the $(J/\psi)/\rho^0$ ratio with increasing Q^2 is observed, although the ratio is below the SU(4) value even at the largest Q^2 . A QCD-based model [12] is in agreement with this behaviour.

9 Conclusions

The reaction $ep \rightarrow ewp$ has been studied in the $e\pi^+\pi^-\pi^0p$ final state for $3 < Q^2 < 20$ GeV², $40 < W < 120$ GeV and $|t| < 0.6$ GeV². The cross-sections $\sigma_{ep \rightarrow ewp}$ and $\sigma_{\gamma^*p \rightarrow \omega p}$ have been measured for the first time at high Q^2 . In addition, the cross-sections $\sigma_{ep \rightarrow e\phi p}$ and $\sigma_{\gamma^*p \rightarrow \phi p}$ have been measured using the same final state.

The cross-section ratio $\omega/\phi = 0.49 \pm 0.15(stat.) \pm 0.12(syst.)$, obtained with the present data, is consistent with the SU(4) expectation.

For the light vector mesons, ρ^0 , ω and ϕ , the cross-section ratios are consistent with the SU(4) expectation for $Q^2 \gtrsim 6$ GeV². The ϕ/ρ^0 cross-section ratio is suppressed at lower values of Q^2 , while the ω/ρ^0 ratio shows no dependence on Q^2 . The $(J/\psi)/\rho^0$ ratio, on the other hand, is a factor of two below that of the SU(4) expectation even at

⁴The recent H1 measurements on ρ^0 and J/ψ electroproduction [19, 22] are not displayed in Fig. 4 since the $(J/\psi)/\rho^0$ cross-section ratios with systematic uncertainties were not published.

Q^2 of 13 GeV², although it is rising rapidly with Q^2 . These observations are consistent with a production mechanism that becomes flavour independent at a sufficiently high Q^2 .

10 Acknowledgements

We thank the DESY Directorate for their strong support and encouragement, and the HERA machine group for their diligent efforts. We are grateful for the support of the DESY computing and network services. The design, construction and installation of the ZEUS detector have been made possible owing to the ingenuity and effort of many people from DESY and home institutes who are not listed as authors. It is also a pleasure to thank M. Strikman for many useful discussions.

References

- [1] T.H. Bauer et al., Rev. Mod. Phys. 50 (1978) 261, Erratum ibid. 51 (1979) 407
- [2] R.M. Egloff et al., Phys. Rev. Lett. 43 (1979) 657 ;
R.M. Egloff et al., Phys. Rev. Lett. 43 (1979) 1545 ;
D. Aston et al., Nucl. Phys. B209 (1982) 56
- [3] ZEUS Collaboration, M. Derrick et al., Z. Phys. C69 (1995) 39 ;
H1 Collaboration, S. Aid et al., Nucl. Phys. B463 (1996) 3 ;
ZEUS Collaboration, M. Derrick et al., Z. Phys. C73 (1997) 253
- [4] ZEUS Collaboration, J. Breitweg et al., Eur. Phys. J. C2 (1998) 247
- [5] ZEUS Collaboration, M. Derrick et al., Z. Phys. C73 (1996) 73
- [6] ZEUS Collaboration, M. Derrick et al., Phys. Lett. B377 (1996) 259
- [7] ZEUS Collaboration, J. Breitweg et al., Z. Phys. C75 (1997) 215
- [8] H1 Collaboration, C. Adloff et al., DESY Report 00-037 (2000) , to be published in Phys. Lett. B
- [9] J.J. Sakurai, Phys. Rev. Lett. 22 (1969) 981
- [10] P.D.B. Collins, *An Introduction to Regge Theory and High Energy Physics* (Cambridge University Press, 1977)
- [11] S. J. Brodsky et al., Phys. Rev. D50 (1994) 3134
- [12] L. Frankfurt et al., Phys. Rev. D54 (1996) 3194
- [13] W. Köpf et al., in *Proceedings of the Workshop on Future Physics at HERA*, edited by G. Ingelman et al. (DESY, Hamburg, Germany, 1996), p. 674, and references therein
- [14] J. C. Collins, L. Frankfurt and M. Strikman, Phys. Rev. D56 (1997) 2982
- [15] M. G. Ryskin, Z. Phys. C57 (1993) 89
- [16] M. G. Ryskin et al., Z. Phys. C76 (1997) 231
- [17] A.D. Martin, M.G. Ryskin, and T. Teubner, Phys. Rev. D55 (1997) 4329
- [18] ZEUS Collaboration, J. Breitweg et al., Eur. Phys. J. C6 (1999) 603
- [19] H1 Collaboration, C. Adloff et al., Eur. Phys. J. C13 (2000) 371
- [20] ZEUS Collaboration, M. Derrick et al., Phys. Lett. B380 (1996) 220
- [21] H1 Collaboration, C. Adloff et al., DESY Report 00-070 (2000) , submitted to Phys. Lett. B
- [22] H1 Collaboration, C. Adloff et al., Eur. Phys. J. C10 (1999) 373

- [23] ZEUS Collaboration, J. Breitweg et al., Phys. Lett. B437 (1998) 432
- [24] ZEUS Collaboration, M. Derrick et al., *The ZEUS Detector*, Status Report, 1993
- [25] M. Derrick et al., Nucl. Instr. and Meth. A309 (1991) 77 ;
A. Andresen et al., Nucl. Instr. and Meth. A309 (1991) 101 ;
A. Bernstein et al., Nucl. Instr. and Meth. A336 (1993) 23
- [26] N. Harnew et al., Nucl. Instr. and Meth. A279 (1989) 290 ;
B. Foster et al., Nucl. Phys. Proc.-Suppl. B32 (1993) 181 ;
B. Foster et al., Nucl. Instr. and Meth. A338 (1994) 254
- [27] ZEUS Collaboration, M. Derrick et al., Z. Phys. C63 (1994) 391 ;
J. Andrusków et al., DESY Report 92-066 (1992)
- [28] K. Muchorowski, Ph.D. thesis, Warsaw University, 1998, (unpublished)
- [29] A. Kwiatkowski, H. Spiesberger and H.-J. Moehring, in *Proceedings of the Workshop on Physics at HERA*, edited by W. Buchmüller and G. Ingleman (DESY, Hamburg, Germany, 1991), p. 1294
- [30] M. Arneodo, L. Lamberti, and M. Ryskin, Comp. Phys. Comm. 100 (1996) 195
- [31] Particle Data Group, C. Caso et al., Eur. Phys. J. C3 (1998) 1.

Reaction	Cross section [nb] ($Q^2 = 7 \text{ GeV}^2, W = 70 \text{ GeV}$)
$\gamma^* p \rightarrow \omega p$	$8.5 \pm 1.1 \pm 2.0$
$\gamma^* p \rightarrow \phi p$	$17.3 \pm 5.0 \pm 6.0$
$\gamma^* p \rightarrow \rho^0 p$	$95 \pm 9 \pm 5$
Cross-section ratio ($Q^2 = 7 \text{ GeV}^2, W = 70 \text{ GeV}$)	
$\sigma_{\gamma^* p \rightarrow \omega p} / \sigma_{\gamma^* p \rightarrow \phi p}$	$0.49 \pm 0.15 \pm 0.12$
$\sigma_{\gamma^* p \rightarrow \omega p} / \sigma_{\gamma^* p \rightarrow \rho^0 p}$	$0.089 \pm 0.014 \pm 0.019$
$\sigma_{\gamma^* p \rightarrow \phi p} / \sigma_{\gamma^* p \rightarrow \rho^0 p}$	$0.182 \pm 0.055 \pm 0.061$

Table 1: Exclusive electroproduction cross-section measurements and ratios for ω , ϕ , and ρ^0 mesons at $Q^2 = 7 \text{ GeV}^2$ and $W = 70 \text{ GeV}$. The ρ^0 cross section is taken from a previous ZEUS publication [18]. The first uncertainty is statistical, the second systematic.

W [GeV]	50	70	100
Number of events	34	30	59
$\sigma_{\gamma^* p \rightarrow \omega p}(Q^2 = 7 \text{ GeV}^2)$ [nb]	$6.2 \pm 1.5 \pm 1.8$	$8.0 \pm 2.1 \pm 2.4$	$12.3 \pm 2.5 \pm 3.6$

Table 2: Exclusive ω production cross sections for $|t| < 0.6 \text{ GeV}^2$ and $Q^2 = 7 \text{ GeV}^2$, measured at three W values. The first uncertainty is statistical, the second systematic.

Q^2 [GeV 2]	$\simeq 0$	3.5	13
$\sigma_{\gamma^* p \rightarrow \omega p}$ [nb]	$1210 \pm 120 \pm 230$	$34.2 \pm 6.8 \pm 8.6$	$2.04 \pm 0.36 \pm 0.68$
$\sigma_{\gamma^* p \rightarrow \rho^0 p}$ [nb]	$11400 \pm 300^{+1000}_{-1200}$	$376 \pm 27^{+19}_{-25}$	$24 \pm 3 \pm 2$
$\sigma_{\gamma^* p \rightarrow \omega p} / \sigma_{\gamma^* p \rightarrow \rho^0 p}$	$0.106 \pm 0.011 \pm 0.016$	$0.091 \pm 0.019 \pm 0.020$	$0.085 \pm 0.018 \pm 0.027$

Table 3: Cross-section measurements and ratios for exclusive production of ω and ρ^0 mesons at three Q^2 values. The ratios at $Q^2 \simeq 0 \text{ GeV}^2$ were calculated using photoproduction cross sections for ω at $W = 80 \text{ GeV}$ [5] and for ρ^0 at $W = 75 \text{ GeV}$ [4], whereas the cross sections at higher Q^2 are for $W = 70 \text{ GeV}$. The ρ^0 production cross sections at high Q^2 are taken from a previous ZEUS publication [18]. The first uncertainty is statistical, the second systematic.

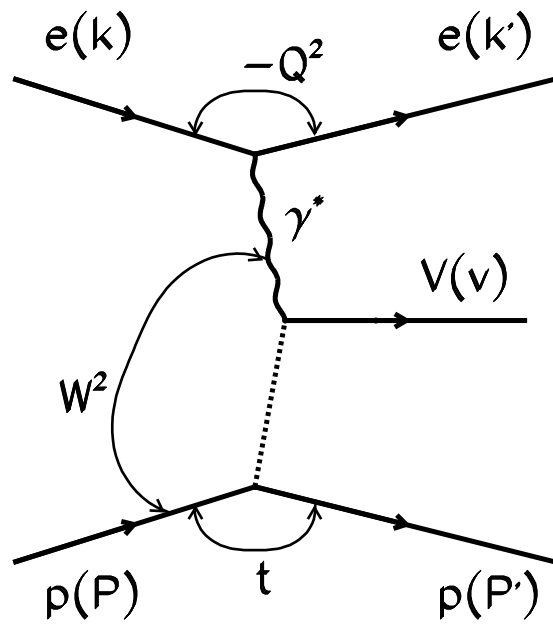


Figure 1: Schematic diagram of exclusive vector-meson electroproduction in e^+p interactions, $ep \rightarrow eVp$. In this analysis, V is either an ω or ϕ meson.

ZEUS 1996 - 1997

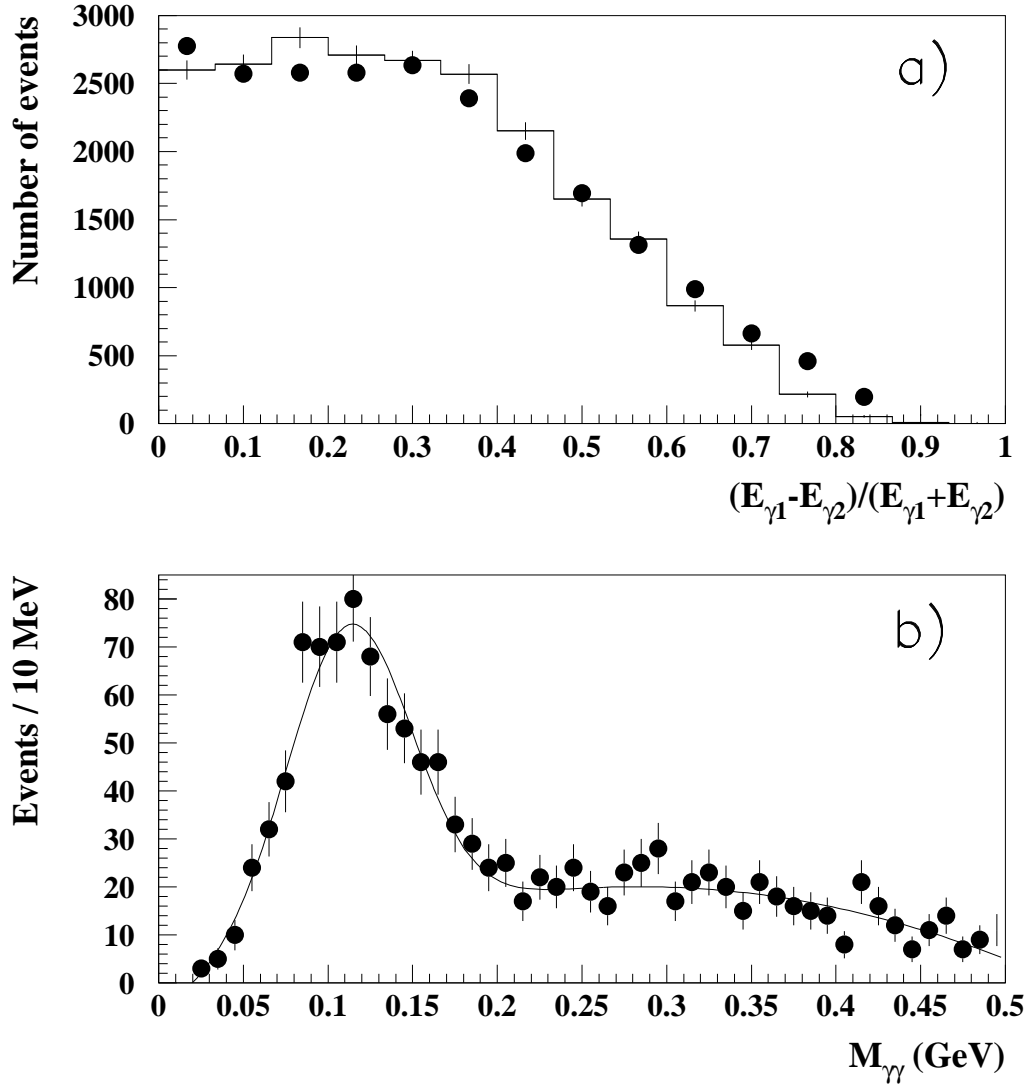


Figure 2: a) The ratio $(E_{\gamma 1} - E_{\gamma 2}) / (E_{\gamma 1} + E_{\gamma 2})$ for π^0 candidates (solid points), where $\gamma 1$ is the more energetic photon candidate. The histogram corresponds to the MC simulation described in the text. The vertical bars on the histogram correspond to the statistical uncertainties of the MC. The statistical uncertainties of the data are smaller than the size of the solid points. b) The invariant-mass spectrum for two photons (solid points). The line represents a fit to the sum of a Gaussian and a second-order polynomial as described in the text.

ZEUS 1996 - 1997

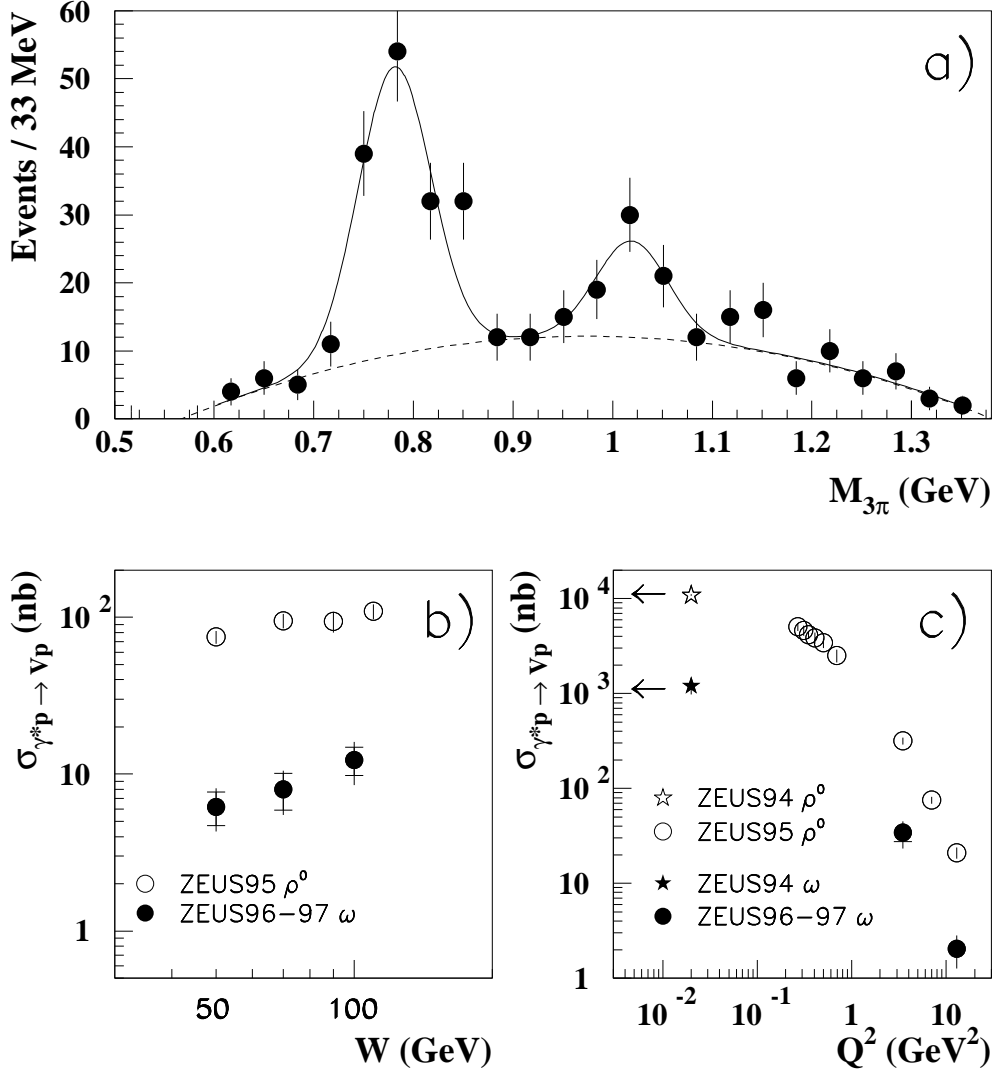


Figure 3: a) The $\pi^+\pi^-\pi^0$ invariant-mass spectrum (solid points). The two peaks correspond to the ω and ϕ mesons. The full line shows the result of the fit explained in the text. The dashed line shows the fitted background. b) The dependence of $\sigma_{\gamma^*p \rightarrow v_p}$ on W at $Q^2 = 7 \text{ GeV}^2$. The full circles are the results from this analysis, and the open circles are from the ZEUS ρ^0 data [18]. c) The dependence of $\sigma_{\gamma^*p \rightarrow v_p}$ on Q^2 at $W = 70 \text{ GeV}$. The results from this analysis are shown as full circles, while the full star is the photoproduction result [5]. The open circles and star are ZEUS results on the ρ^0 cross sections at $W = 50 \text{ GeV}$ [4, 18].

ZEUS 1996 - 1997

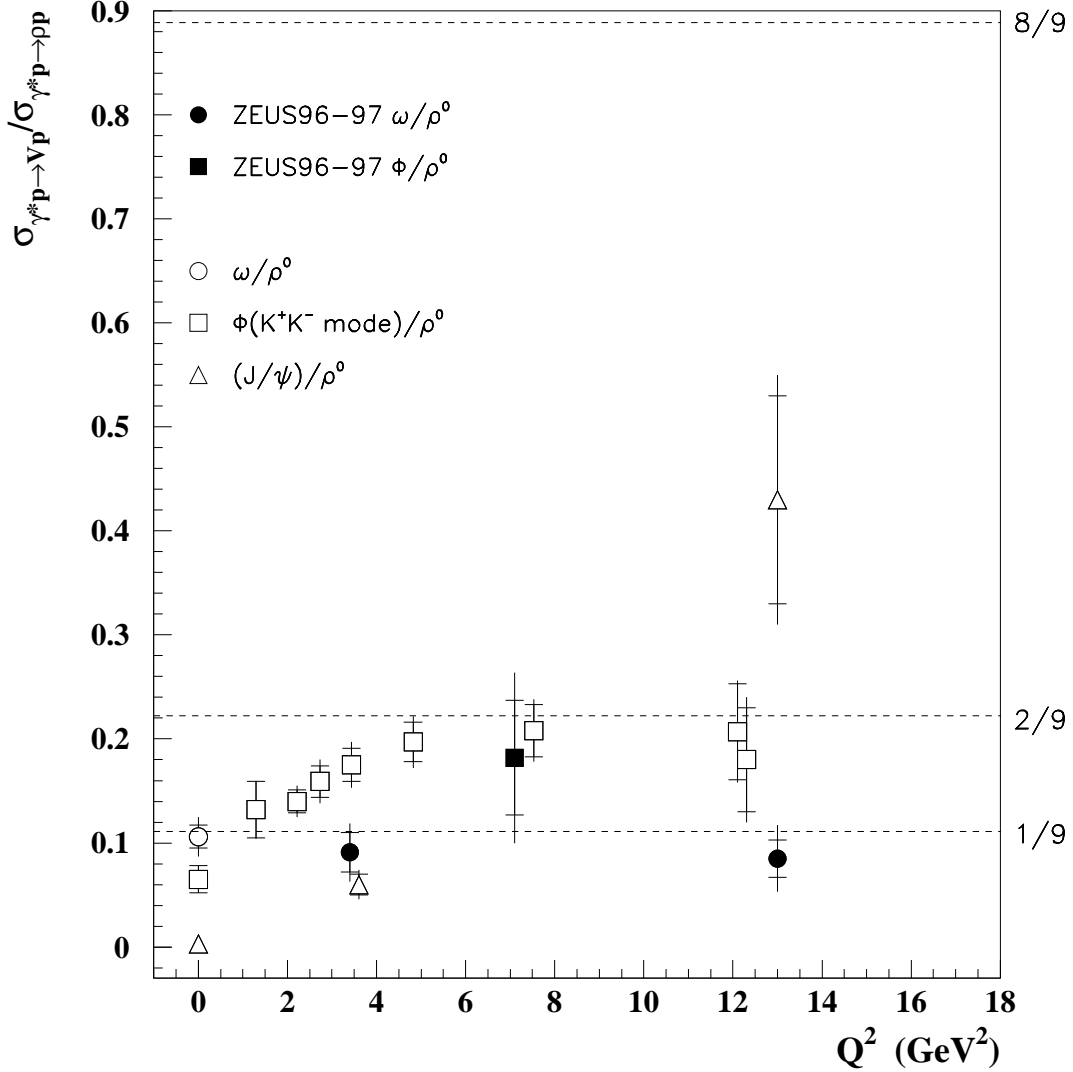


Figure 4: The ratios of the ω , ϕ and J/ψ exclusive cross sections to those for the ρ^0 meson as a function of Q^2 . The ω/ρ^0 and ϕ/ρ^0 results from this analysis are shown with full symbols. The ω/ρ^0 photoproduction point (open circle) was calculated using the measured cross sections from previous ZEUS publications [5] and [4]. Open squares at $Q^2 \simeq 0 \text{ GeV}^2$ [6] and $Q^2 = 12.3 \text{ GeV}^2$ [20] represent the ZEUS ϕ/ρ^0 cross-section ratios, while the others represent the H1 ϕ/ρ^0 ratios [21]; for both the ZEUS and H1 measurements, the $\phi \rightarrow K^+ K^-$ channel was used. Triangles represent the $(J/\psi)/\rho^0$ cross-section ratios [7,18]. The horizontal dashed lines correspond to the SU(4) expectations.